Growth and characterization of GaAs/$In_xGa_{1-x}As$/GaAs axial nanowire heterostructures with symmetrical heterointerfaces*

Lü Xiao-Long(吕晓龙), Zhang Xia(张 霞)†, Liu Xiao-Long(刘小龙), Yan Xin(颜 鑫), Cui Jian-Gong(崔建功), Li Jun-Shuai(李军帅), Huang Yong-Qing(黄永清), and Ren Xiao-Min(任晓敏)

State Key Laboratory of Information Photonics & Optical Communications, Beijing University of Posts and Telecommunications, Beijing 100876, *China*

(Received 22 August 2012; revised manuscript received 27 November 2012)

We report on the Au-assisted vapour–liquid–solid (VLS) growth of GaAs/$In_xGa_{1-x}As$/GaAs ($0.2 \leq x \leq 1$) axial double-heterostructure nanowires on GaAs (111) B substrates via the metal–organic chemical vapor deposition (MOCVD) technique. The influence of the indium (In) content in an Au particle on the morphology of nanowires is investigated systematically. A short period of pre-introduced In precursor before the growth of $In_xGa_{1-x}As$ segment, coupled with a group III precursor interruption, is conducive to obtaining symmetrical heterointerfaces as well as the desired In/Ga ratio in the $In_xGa_{1-x}As$ section. The nanowire morphology, such as kinking and tapering, are thought to be related to the In composition in the catalyst alloy as well as the VLS growth mechanism.

Keywords: nanostructures, nanowire heterostructures, metal–organic chemical vapor deposition

PACS: 61.46.Hk, 68.37.Lp, 61.46.Km **DOI:** 10.1088/1674-1056/22/6/066101

1. Introduction

The semiconductor nanowires (NWs) that have aroused the great interest of researchers lie in their potential applications in electronics and optoelectronics. Due to the unique one-dimensional (1D) physical properties, such as direct bandgap and high electron mobilities, III–V semiconductor NWs are ideal building blocks for future optoelectronic devices. Based on the conventional vapor–liquid–solid (VLS) mechanism,[1] desired growth of axial and radial heterostructured NWs can be achieved by tuning the precursor influx under different growth temperatures.[2] In the case of axial GaAs/$In_xGa_{1-x}As$/GaAs NWs, structural and optical properties have been studied.[3] The bandgap of $In_xGa_{1-x}As$ is modulated by adjusting the mole fractions between the group III materials.[4]

Since the NW growth is mediated by the composition of alloy particles, many extraordinary physical phenomena can be observed compared with their two-dimensional (2D) counterparts, such as graded heterointerfaces[5] and kinked (or branched) NWs.[6] Three main issues for the growth of axial heterostructures are as follows: (i) the growth of vertical free-standing NWs; (ii) NWs with a high-quality crystal structure; (iii) a sharp interface between the two lattice-mismatched materials. It is well known that due to the interfacial energy of Au/GaAs lower than that of Au/InAs, the axial growth of InAs on GaAs NW is a failure.[6] Moreover, for the axial growth of GaAs/InGaAs/GaAs NWs, an interruption of an In precursor prior to and after the InGaAs growth, showed a high In composition gradient at the heterojunctions.[7] However, the transitional length between GaAs/InGaAs and that between InGaAs/GaAs are not equal. And the symmetry of the heterointerfaces is a key issue for NW heterostructures and relevant devices.

In this paper, we systematically investigate the morphological, compositional and structural characteristics of GaAs/$In_xGa_{1-x}As$/GaAs ($0.2 \leq x \leq 1$) axial double-heterostructured NWs. It is found that the morphology of NWs is closely related to the composition in the catalyst, which also determines the incorporation of In in an $In_xGa_{1-x}As$ segment. Besides a precursor interruption, a short period of In precursor before the formation of the middle $In_xGa_{1-x}As$ segment can sensitively affect the symmetry of the heterostructure interfaces. The sharpness and symmetry of the heterointerfaces are also investigated in detail.

2. Experimental procedure

The Au-assisted VLS growth was performed in a Thomas Swan close coupled showerhead-metalorganic chemical vapor deposition (CCS-MOCVD) system at a total pressure of 1.33×10^4 Pa with hydrogen serving as the carrier gas. Trimethylgallium (TMGa), trimethylindium (TMIn), and arsine (AsH_3) were used as precursors. The five samples of GaAs/$In_xGa_{1-x}As$/GaAs NWs grew in the following sequence. i) A layer of Au film with a thickness of 4 nm was deposited on an epi-ready GaAs (111) B substrate by magnetron sputtering. Then the Au-coated wafer was loaded into

*Project supported by the National Basic Research Program of China (Grant No. 2010CB327600), the National Natural Science Foundation of China (Grant Nos. 61020106007 and 61077049), the International Science & Technology Cooperation Program of China (Grant No. 2011DFR11010), the Specialized Research Fund for the Doctoral Program of Higher Education (Grant No. 20120005110011), and the 111 Program of China (Grant No. B07005).

†Corresponding author. E-mail: xzhang@bupt.edu.cn

© 2013 Chinese Physical Society and IOP Publishing Ltd

the MOCVD chamber and annealed at 650 °C for 5 min in arsine and hydrogen ambient for the desorption of surface contaminants and formation of eutectic Au–Ga alloy droplets as a catalyst. ii) After cooling down to 440 °C the GaAs segment was grown for 200 s with a TMGa flow rate of 38.6 μmol/min. The flow rate of AsH_3 was kept constantly at 4.46×10^3 μmol/min during all the NWs heterostructures growth and maintained until the reactor was cooled down to 280 °C. iii) TMIn was introduced for 100 s to form the axial $In_xGa_{1-x}As$ segment. TMGa and TMIn flow rates were tuned to keep a constant V/III ratio of 116 the same as that in step ii), and the TMIn/(TMGa + TMIn) ratio varied linearly from 0.2 to 1. iv) The growth condition for the upper GaAs segment is the same as that in step ii). Before and after formation of the middle $In_xGa_{1-x}As$ insert, a 3-min growth interrupt was included to adjust the group III precursors. The corresponding growth temperature was 420 °C. The schematic diagram of the NW heterostructures is shown in Fig. 1. For all the samples, TMIn was switched 2 s earlier than TMGa for the formation of the InGaAs section in order to obtain symmetrical heterointerfaces. The above growth conditions were previously optimized for obtaining untapered and pure ZB structured GaAs NWs.[8]

The fabricated NW heterostructures were characterized by a HITACHI S-5500 field-emission scanning electron microscope (SEM) with an accelerating voltage of 5.0 kV. Transmission electron microscope (TEM) and energy dispersion spectrum (EDS) investigations were carried out using a JEOL-2100F instrument operating at 200 kV. For TEM specimen preparation, NWs were removed from the wafer by ultrasonicating the samples in ethanol for 5 min, followed by dispersing the suspension droplets onto a holy carbon/Cu grid. For photoluminescence (PL) measurements, NWs were left on the substrate. The excitation source was a laser with a wavelength of 510 nm.

3. Results and discussion

Cross-sectional view SEM images of the as-grown GaAs/$In_xGa_{1-x}As$/GaAs axial heterostructures NWs with a desired IN content $x = 1$, 0.8, 0.6, 0.4, and 0.2 (sample A, B, C, D, and E) are shown in Figs. 1(a)–1(e), respectively. For sample A, there are only about 3%∼4% of the NWs grown vertically on the substrate. For sample B, nearly all the NWs are kinked compared with those for sample A, except those with diameters more than 500 nm. The NW lengths of both samples C and D are both 4.5 μm, while the NW length of sample E is 4.7 μm. It is obvious that with the decrease of In content incorporated into the $In_xGa_{1-x}As$ segment, the proportion of vertically free-standing NWs increases. It seems that for all the samples, only the upper GaAs parts are tapered for thin NWs. These phenomena may be explained by the VLS growth mechanism in combination with the effective V/III ratio in the catalyst droplet.

We observe that nearly all the NWs are kinked, when the desired In content is $x = 1$, in the middle $In_xGa_{1-x}As$ section for sample A. A similar phenomenon has been observed for the growth of InAs on the top of GaAs.[6] And it has been well explained in terms of interface energy as follows: due to the interface energies $\gamma_{Au/InAs} \geq \gamma_{Au/GaAs} + \gamma_{In/GaAs}$ and the fact that In atoms are easily mobile with a strong segregation behavior, the system tends to create kinked NWs.[6] In our case, the interface energy is determined by the compositions of the catalyst alloy, which is closely related to the incorporation of In content during the growth of the middle $In_xGa_{1-x}As$ segment. For sample B, even more NWs are kinked than for sample A. This might be due to the inhomogeneous composition of a liquid catalyst. Both the low level of gallium content and the strong segregation behavior of In may lead to a strong composition inhomogeneity in the catalyst alloy. Moreover, In has a low surface energy (compared to Au). A large portion of In content in the catalyst alloy changes the droplet size and therefore may wet the sidewalls which results in the VLS growth becoming unstable and tending to create kinked NWs.[9,10]

Only the upper GaAs parts are tapered for thinner NWs. The traditional view is that the tapering effect of NWs is mainly caused by lateral growth of adatoms at an elevated temperature.[11] However, our growth temperature is relatively low and the growth condition is optimized for the growth of untapering NWs.[8] Paladugu *et al.*[12] have shown that In could still be detected in the alloy particle after 3 min of GaAs growth. When growing the upper GaAs segment, residual In incorporated into the catalyst during the middle $In_xGa_{1-x}As$ step, influences the supersaturation of Ga in the catalyst, and changes the effective V/III molar ratio in the catalyst alloy. Thus, the tapering effect may also be closely related to the effective V/III molar ratio in the catalyst droplet.

For an analysis of the axial component of the as-grown NWs, an EDS study is carried out on the individual NW. There are 2 specimens to be examined for each sample. The bright field TEM with EDS images in Figs. 2(a), 2(c), and 2(d) indicate that GaAs/InGaAs/GaAs heterostructures have sharp symmetrical interfaces. The width for the variation of the In intensity profile from 10% to 90% across the interface shows that both the two heterointerfaces share the same composition gradient with lengths of 48, 80, and (41±5) nm for samples A, D, and E, respectively. And the half width at half maximum (HWHM) of the In EDS profile on each side of the interfacial region displays that the total lengths of $In_xGa_{1-x}As$ section are 273, 169, and (109±5) nm for samples A, D, and E, respectively (as shown by the

shaded areas in Fig. 2). While figure 2(b) shows that, for GaAs/$In_{0.6}Ga_{0.4}As$/GaAs NWs (sample C), the GaAs/InGaAs heterointerface is sharper ((51±5) nm) than the InGaAs/GaAs heterointerface ((282±5) nm). This may be due to the fact that the 2-s early introduced large amount of In precursor leads to the asymmetrical heterointerfaces. To obtain a symmetrical heterointerface for sample B and to further understand the effect of the early introduced In precursor on the NW heterostructure, another sample (sample F) was prepared by reducing the early introduced In procersor amount and the early reduced In amount is set to be the same as that for sample D. Figure 2(e) shows that the length of the InGaAs segment for sample E is (84±5) nm, and the widths of the two symmetrical heterointerfaces are both (41±5) nm. It is worthwhile to note that the EDS scan for sample B is not carried out due to the fact that nearly all NWs are kinked.

It is well known that when growing GaAs/$In_xGa_{1-x}As$/GaAs axial double-heterostructures NWs, the two heterointerfaces are not symmetrical. The occurrence of the transition region is well explained by the higher affinity of In than that of Ga in the Au–In–Ga catalyst system.[13,14] When the middle $In_xGa_{1-x}As$ segment grows onto the lower GaAs part, the gold seed particle accumulates a larger amount of Ga than that of In, which leads to a lower In/Ga ratio in the beginning of the $In_xGa_{1-x}As$ segment than expected. According to Bauer's report, the group III precursor growth interrupt prior to and after the middle $In_xGa_{1-x}As$ growth can obtain evident composition gradients at the heterojunctions.[7] However, the two interfaces seem not to be symmetrically sharp. While symmetrical heterostructure interface is indispensable when thin barriers are to be fabricated inside the NWs. In the experiments, we find that a 2-s earlier switched-on In precursor at the beginning of the formation the $In_xGa_{1-x}As$ segment in combination with the judicious choice of its flow rate, can obtain a NW heterostructure with symmetrical heterointerfaces. The early introduced In precursor prior to the $In_xGa_{1-x}As$ segment growth can compensate the hysteresis of In incorporation in the eutectic alloy.

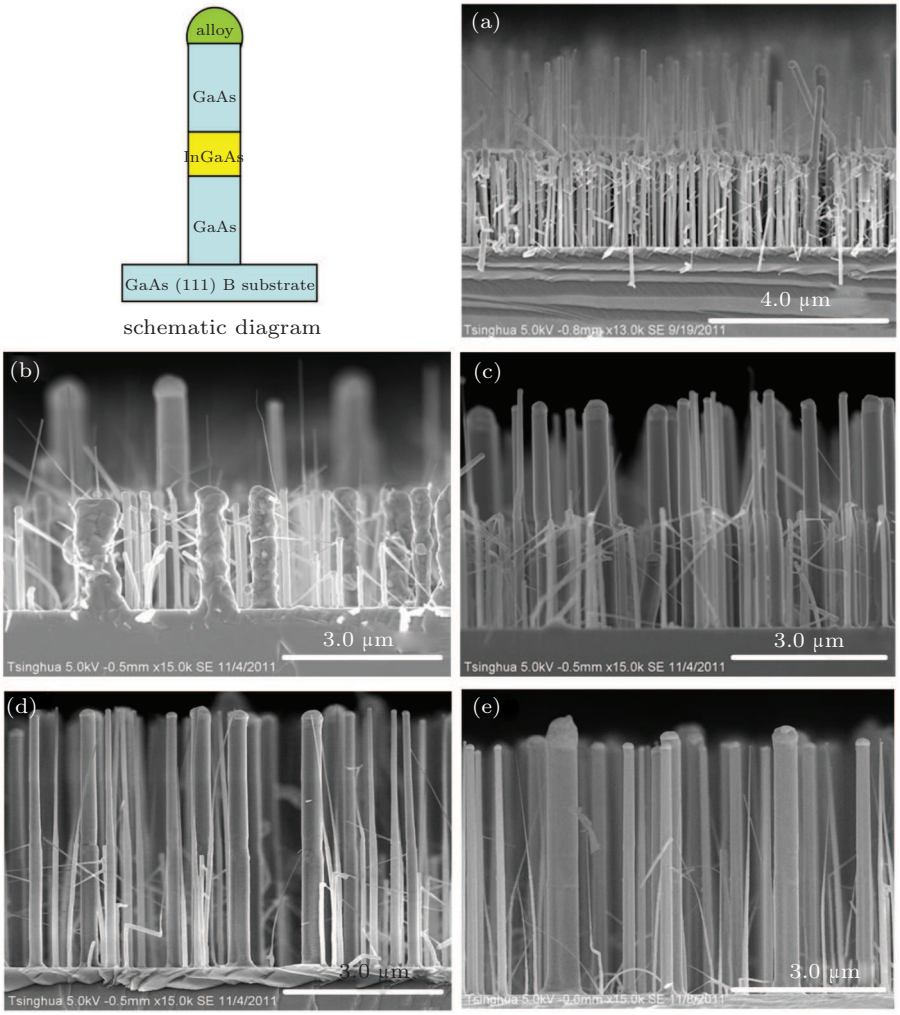


Fig. 1. (color online) Schematic diagram and SEM micrographs of GaAs/$In_xGa_{1-x}As$/GaAs double-heterostructures NWs on GaAs (111) B substrate , with $x = 1$ (a), 0.8 (b), 0.6 (c), 0.4 (d), and 0.2 (e).

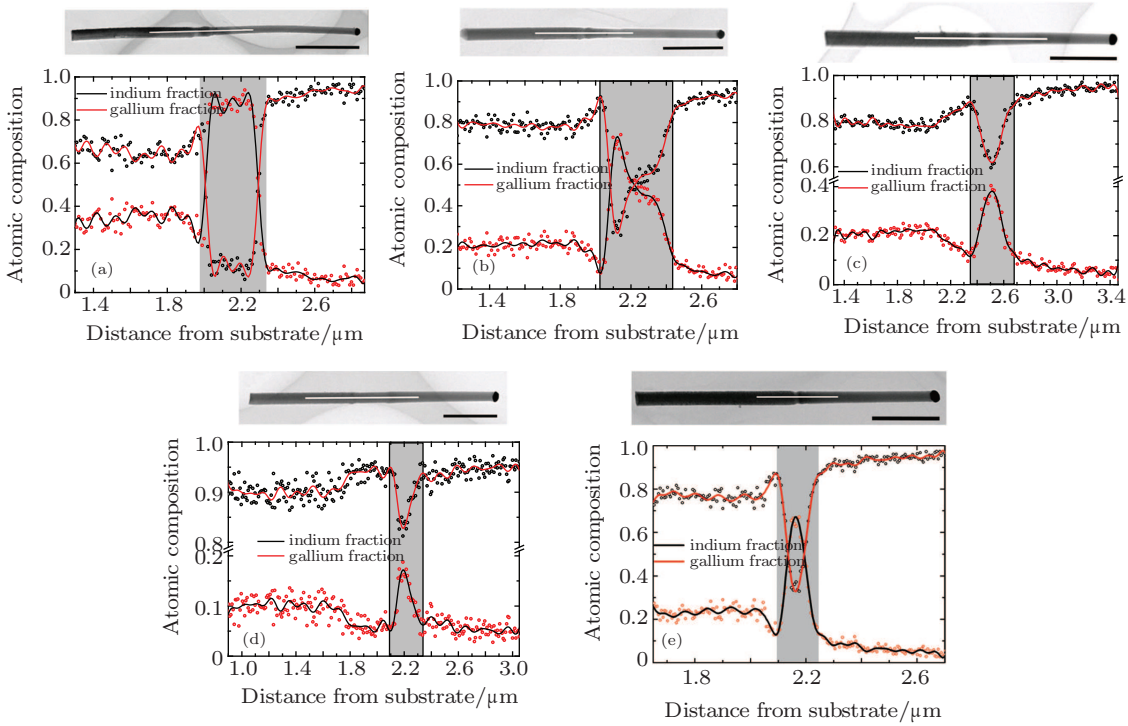


Fig. 2. (color online) Intensity calibrated EDS line scan along the $In_xGa_{1-x}As$ section of a single NW, with $x = 1$ (a), 0.6 (b), 0.4 (c), 0.2 (d), and 0.6 (e) (with the amount of pre-introduced In changed), corresponding to samples A, C, D, E, and F, respectively. The size of scale bar is 1 μm.

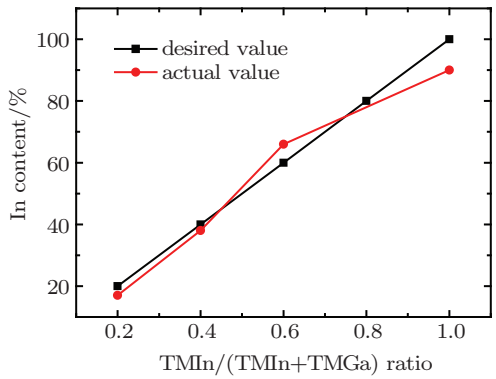


Fig. 3. (color online) Desired and actual (EDS) values of the In content in $In_xGa_{1-x}As$ segment.

As can be seen from Fig. 2, for all the samples, the In content of the lower GaAs part is larger than that of the corresponding upper part. This is because during the formation of the middle $In_xGa_{1-x}As$ section, there is an unintended $In_xGa_{1-x}As$ lateral growth along the lower part of GaAs segment.[5] Both the impingement of growing species directly on the side walls and the diffusion of adatoms from the substrate to the lateral surface result in the GaAs core encapsulated by an $In_xGa_{1-x}As$ shell. In addition, the early introduced In precursor can significantly change the actual In/Ga ratio in the $In_xGa_{1-x}As$ segment. Figure 3 shows the comparison between the In/(In+Ga) desired values and actual values. For samples C and E, the desired In/(In+Ga) ratio values change from 0.6 and 0.2 to 0.67 and 0.17, respectively. For sample D, the actual value is in line with the desired value.

For a better understanding of the structural properties and radial chemistry of the NWs, TEM with EDS studies are carried out on the individual NW. The bright field TEM images of the NW are taken along the $[1\bar{1}0]$ zone axis under the incident electron beam. Figure 4 shows the TEM analyses of three different parts of sample C. The main crystallographic structure is of zinc blende (ZB). For the upper part, it shows a pure GaAs ZB structure (see the EDS scan image in Fig. 4(d)). There are only a few stacking faults just below the alloy particle. The high-resolution TEM image and the corresponding Fourier transformation of the crystallographic structure confirm a few defects in the middle InGaAs heterostructured section and the crystal orientation change in the lateral boundary. The growth condition of the middle segment, such as high V/III ratio and relatively low growth temperature, may all contribute to such defects.[15] The composition fluctuation and size change of the catalyst droplet will also lead to the formation of stacking faults or twins in the NWs. Moreover, the composition fluctuation can also change the supersaturation and tension of the droplet.[16,17] The lower part shows pure ZB GaAs segment encapsuled by an $In_xGa_{1-x}As$ shell with the In content around $x = 0.6$, (see the EDS scan image in Fig. 4(e)). The $In_xGa_{1-x}As$ shell only has a few stacking faults (see the arrows shown in Fig. 4(c)). This is due to the fact that the large lateral interface between GaAs core and $In_xGa_{1-x}As$ shell can release stress effectively.

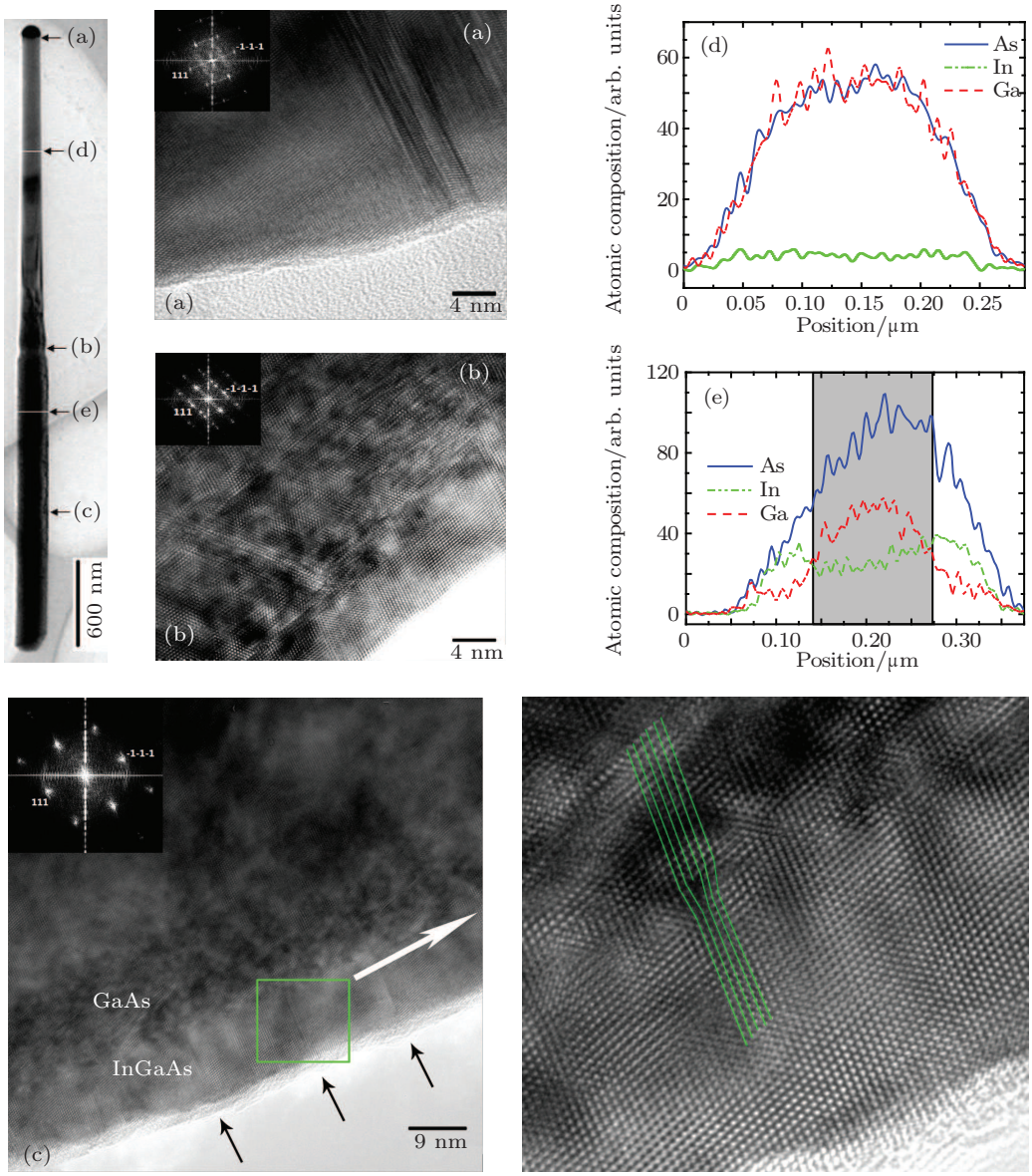


Fig. 4. (color online) TEM with radial EDS line scan on an individual NW of sample C of the upper part (a), the middle part (b), and the lower part (c); radial EDS scan of upper (d), and lower part (e). The Fourier transform of the structures were shown in insets, correspondingly.

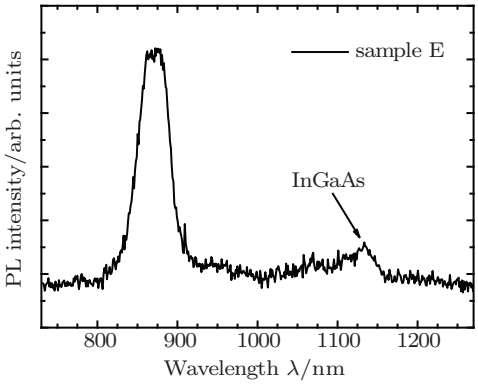


Fig. 5. PL spectrum of GaAs/$In_{0.2}Ga_{0.8}As$/GaAs axial double heterostructure NWs.

To investigate the optical properties of the grown structures, the PL spectral measurement for sample E is performed at room temperature. As shown in Fig. 5, a high-intensity PL signal confirms a good crystalline quality. Besides the GaAs band gap peaks around 870 nm and 880 nm, the middle $In_{0.2}Ga_{0.8}As$ segment peak is observed at a higher wavelength around 1130 nm. It is worthwhile to note that there is no InGaAs signal detected for the original sample E. In order to passivate surface state on the NW surface and suppress nonradiative recombination, the NWs of sample E are encapsulated by an AlGaAs shell.[18]

4. Conclusion

We systematically investigated the Au-assisted formation of GaAs/$In_xGa_{1-x}As$/GaAs axial double heterostructure NWs via the VLS mode. At the optimized low growth temperature, the kinking and tapering effects of the NWs are believed to be related to the In content in the catalyst alloy. The crystal

structure and spatial localization of GaAs/$In_xGa_{1-x}As$/GaAs heterostructure are studied by TEM with an EDS line scan. In addition to the group III precursor interrupt, the symmetry of the heterointerfaces and the actual In/(Ga+In) ratio in the $In_xGa_{1-x}As$ section, are sensitive to the early introduced In precursor. This work is important for further developing the NW heterostructures and relevant devices.

References

[1] Wagner R S and Ellis W C 1964 *Appl. Phys. Lett.* **4** 89

[2] Hiruma K, Tomioka K, Mohan P, Yang L, Noborisaka J, Hua B, Hayashida A, Fujisawa S, Hara S, Motohisa J and Fukui T 2012 *Journal of Nanotechnology* **2012** 1

[3] Panev N, Persson A I, Skold N and Samuelson L 2003 *Appl. Phys. Lett.* **83** 2238

[4] Porod W and Ferry D K 1983 *Phys. Rev. B* **27** 2587

[5] Regolin I, Sudfeld D, Lüttjohann S, Khorenko V, Prost W, Kästner J, Dumpich G, Meier C, Lorke A and Tegude F J 2007 *J. Cryst. Growth* **298** 607

[6] Paladugu M, Zou J, Guo Y N, Auchterlonie G J, Kim Y, Joyce H J, Gao Q, Tan H H and Jagadish C 2007 *Small* **3** 1873

[7] Bauer J, Gottschalch V, Paetzelt H and Wagner G 2008 *J. Crystal Growth* **310** 5106

[8] Huang H, Ren X M, Ye X, Guo J W, Wang Q, Yang Y S, Cai S W and Huang Y Q 2010 *Nano Lett.* **10** 64

[9] Dubrovskii V G, Cirlin G E, Sibirev N V, Jabeen F, Harmand J C and Werner P 2011 *Nano Lett.* **11** 1247

[10] Krogstrup P, Curiotto S, Johnson E, Aagesen M, Nygard J and Chatain D 2011 *Phys. Rev. Lett.* **106** 125505

[11] Soci C, Bao X Y, Aplin P R and Wang D L 2008 *Nano Lett.* **8** 4275

[12] Paladugu M, Zou J, Guo Y N, Zhang X, Kim Y, Joyce H J, Gao Q, Tan H H and Jagadish C 2008 *Appl. Phys. Lett.* **93** 101911

[13] Krogstrup P, Yamasaki J, Sørensen C B, Johnson E, Wagner J B, Pennington R, Aagesen M, Tanaka N and Nygard J 2009 *Nano Lett.* **9** 3689

[14] Borg B M, Dick K A, Ganjipour B, Pistol M, Wernersson L E and Thelander C 2010 *Nano Lett.* **10** 4080

[15] Joyce H J, Gao Q, Tan H H, Jagadish C, Kim Y, Zhang X, Guo Y N and Zou J 2007 *Nano Lett.* **7** 921

[16] Bauer J, Gottschalch V, Paetzelt H, Wagner G, Fuhrmann B and Leipner H S 2007 *J. Crystal Growth* **298** 625

[17] Glas F, Harmand J and Patriarche G 2007 *Phys. Rev. Lett.* **99** 146101

[18] Guo J W, Huang H, Ren X M, Yan X, Cai S W, Guo X, Huang Y Q, Wang Q, Zhang X and Wang W 2011 *Chin. Phys. Lett.* **28** 036101